ISSN: 2287-6898
International
Journal of Bio-Pharma Research
Volume 8, Issue 3 (2019) pp. 2504-2513
Research Article Open Access

Performance of Solar cell fabricated using TiO_2: rGO on glass and Si substrates prepared by Thermal Evaporation Technique

Prabhavathi G.[1,4], Anuradha N.[2], Afroos Banu A.[3], Ayeshamariam A.[1,4*], Punithavelan N.[5], Mohamed Saleem A.[6] and M. Jayachandran[7]

[1]Research and Development Center, Bharathidasan University, Tiruchirappalli, 620 024, India.
[2]Department of Physics, Bon Secours College, 613 006, India.
[3]Department of Chemistry, Khadir Mohideen College, Adirampattinam 614 701, India.
[4]Department of Physics, Khadir Mohideen College, Adirampattinam 614 701, India.
[5]Department of Physics Divisions, School of Advanced Sciences (SAS), VIT University Chennai Campus, Chennai, 600 127, India.
[6]Department of Physics, Jamal Mohamed College (Auto), Tiruchirappalli, 620 020, India.
[7]Department of Physics, Sethu Institute of Technology, Pullor, Kariapatti, 625 606, India.

Abstract: TiO_2: rGO doped material is deposited on glass and Si substrates. These hetero nanostructures have multiple applications in photovoltaic because of their charge transport properties. In this study, we prepared tetragonal TiO_2: rGO doped material is deposited on glass and Si substrates (NCs) using Thermal Evaporation method. The morphological properties of the NCs were investigated using X-ray diffraction, Field-emission scanning electron microscopy with EDAX analysis, Atomic force microscopy, and Photovoltaic studies analysis. The results showed that the surface area of the deposited films increased significantly and the anatase TiO_2: rGO doped material is deposited on glass and Si substrates was efficient photovoltaic performance with the other nanocomposites or the bare individual nanoparticles. It may be attributed to the increased active surface area, the increased adsorption of the light and target surface atoms, as well as efficient electron–hole transformation.

Key words: TiO_2: rGO, Si substrates, glass substrates, nanocomposites and adsorption

Introduction

The intensity of solar radiation in free space at the average distance of the earth from the Sun is defined as the solar constant with the value of 1.940 langleys (1.353 W/m²) [1]. Because the earth moves in an elliptical orbit, the value of solar intensity at the upper atmosphere varies by about ±3 percent during the course of a year [2]. Much more significant variation results on the earth's surface because of climatic factors and of course, the day–night cycle due to earth's rotation. Flexible solar cells are one of the most promising technologies to produce the light weight solar cells for space and aerospace applications, portable electronic devices and integrated photovoltaics [3]. Dye-sensitized solar cell (DSSC) converting solar energy into electricity by complicated photo-electrochemical reactions is one of the promising solutions to energy crisis and environmental pollution [4].

First generation solar cell developed in midst of nineteenth century was purely based on silicon-based materials [5]. First generation photovoltaic cells are the dominant technology in the commercial production of solar cells, accounting for more than 86% of the solar cell market. Cells are made using crystalline silica wafer, consists of a large area single layer p-n junction diode. Silicon is the most extensively used material in photovoltaic devices. Silicon is also the second-most plentiful element in the Earth's crust (after oxygen) and is most universally used semiconductor materials which can be easily tunable to p and n type semiconductor. It is a mixture of low raw material cost, comparatively unpretentious processing, and a convenient temperature range makes it presently the best compromise among the various contending photovoltaic materials. Silicon solar cells divided into crystalline and thin films. Monocrystalline Silicon serves as base light absorbing materials for photovoltaics. For thermal solar energy collection is usually a good approximation to assume that the solar spectrum is that of a

Corresponding Author:
Dr. A. Ayeshamariam,
Head, Department of Physics
Khadir Mohideen College Adirampattinam-614701,
Tamilnadu, India.
E-mail: aismma786@gmail.com

5800 K black body [6]. The output of the solar cell however is significantly affected by the details of the spectrum. The principle effects are due to water vapor absorption in the infrared ozone absorption in the ultraviolet and scattering by air borne dust and aerosols. Aerosol scattering varies inversely with the fourth power of the wavelength (which is why the sky appears blue rather than yellow or red). An effective solar cell needs (i) Absorption of a large portion of the incident solar radiation, (ii) the capable collection of both photogenerated electrons and holes, (iii) a junction with a built-in potential on the order of 1V, and (iv) a low internal series resistance [7]. Initial cost of producing monocrystalline silicon and its fragileness remains main disadvantages [8]. Polycrystalline silicon photovoltaic cell, polysilicon (p-Si) and multi-crystalline silicon (mc-Si), were commercialized in early 1980s [9]. The conductivity of solid materials vary over an enormous range representative values are from less than 2 x 10^{-17} mho/m for fused quartz, a good insulator to about 6 x10^{7} mho/m for silver, a good conductor material, with intermediate conductivity values are called semiconductors. And these semiconductors show the best performance under the sunlight during the energy conversion. When protons from the Sun are absorption in a semiconductor, they create free electrons with higher energies than the electrons, which provide the bonding in the base crystals. Once these free electrons are created, there must be an electric field to induce these higher energy electrons to flow out of the semiconductor to do useful work. The electric field in most solar cells is provided by a junction of materials which have different electrical properties. [10].

Graphene, which was discovered in the recent years, is majorly being synthesized by chemical methods for GO compared to all other methods. The main disadvantage of chemical method is the irreversible aggregation of the product graphene oxide and high toxic nature of the reducing agents making it unfit for biological related applications. In order to overcome the aforesaid difficulties, our graphene has been synthesized by green method where we used the extract of plant "*Lawsonia Inermis*" to reduce graphene oxide prepared from graphite powder. This way the graphene does not have toxic impurities in it. Very few reports are available on the reduction of GO by using tea solution, glucose, polyphenol alcohol, wild carrot root, reducing sugar, melatonin, bacteria, vitamin C, amino acid and bovine serum albumin [11].

Materials and Methods

Only at pressures 10^{-5} torr does the mean free path between collisions becoming large enough so that the vapor beam arrives at the substrates unscattered. A low vacuum has an additional effect that the gas molecules strike the substrate and this can result in contamination of the films being deposited. Almost all the materials vaporize a solid or liquid phase as neutral atoms or molecules. The evaporation of materials is done in vacuum system which in most cases comprises a diffusion pump backed by rotary pump. The electrode preparation for photovoltaic studies is shown in Figure 1(a-b).

The pelletized powder particle was deposited on glass and Si substrates. Thermal evaporation technique is the simplest method for a vacuum coating unit was used to perform this technique. It consists of vacuum system, evaporation chamber and heating arrangement. The vacuum system consisted of a rotary pump and diffusion pump. The rotary pump capable of attaining 1×10^{-3} mbar vacuum is used as backing device for diffusion pump which ultimately creates a vacuum in the order of 10^{-5} mbar. The diffusion pump can achieve the vacuum of 10^{-6} mbar. To evaporate the pelletized sample in high vacuum chamber it requires a source in the form of boat to support the sample and to supply heat for vaporization, the sample to be evaporated and a substrate on which the coating has to be done. The source used was Molybdenum (Mo) boat because of it has high melting point and low vapor pressure. TiO_2: rGO doped material deposited on glass and Si substrates were made up of solar cells with giving a final active area of 10-4.5 mm^2. A refractive index matching liquid of nD¼ 1.54 was applied to the solar cell and the layer was pressed on top. There were no air bubbles in the structure, and the layers remained attached to the cell via capillary forces. In photo-anode, generally wide bandgap semiconducting oxides like TiO_2, GO are coated over glass and conducting

substrates it collects the photo-excited electrons and conducts photo-electrons from light to the substrates. The bandgap, composition and morphology of oxides on different substrates as well as the thickness of its layers influence the charge collection, transportation and light harvesting properties.

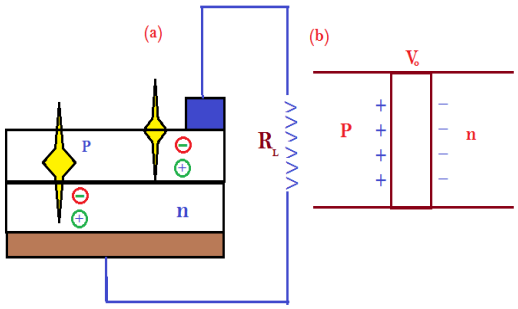

Figure 1(a): P-N junction solar cell with load resistance R_L (b) Formation of the open circuit voltage

The X-ray powder diffraction (XRD) experiments were measured on a RigaKu D/max-RB diffractometer with Ni-filtered graphite monochromatized Cuk_α radiation (λ = 1.54056 Å) under 40 kV, 30 mA and scanning between 10° to 90° (2θ). The morphology was characterized by scanning electron microscopy (SEM, Hitachi, S-4800) and transmission electron microscopy (TEM, Tecnai G2, FEI Company) with X-ray energy dispersive spectrometry (EDS). The surface topography of deposited specimens on glass and Si by Thermal Evaporation Technique were examined by using atomic force microscopy applying tapping mode and the tip is made by silicon nitrate. Histogram analysis of the surface roughness of the coating was measured using nanoscope software (version 4.43r8) and the images were modified using an X-Y plane. Fit auto procedure.

Results and Discussion

The XRD patterns for TiO_2: rGO doped on the glass and TiO_2: rGO doped on the Si thin films deposited are shown in Figure 2a and 2b. Films at higher substrate temperature reveal only an intense diffraction peak around 27°, which corresponds to (100) of the tetragonal phase of TiO_2. From the peak position and the integral width at half maximum of the respective peak, the particle sizes in the TiO_2: rGO doped on the glass (JCPDS file 89-0555) and TiO_2: rGO doped on the Si are calculated; the average crystallite size is estimated from the Debye-Scherrer formula [12], as follows:

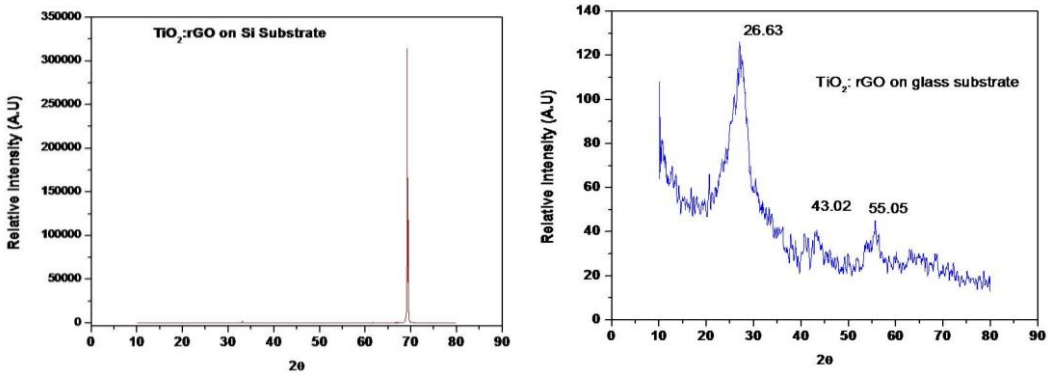

Figure 2(a-b): XRD Analysis of TiO_2: rGO coated on glass and Si substrates

$$D_{XRD} = \frac{0.9\lambda}{\beta \cos\theta}, \text{----------(1)}$$

Where D_{XRD} is the mean particle size, λ = 0.15406 nm is the x-ray wavelength, θ is the Bragg diffraction angle and β is the full width at half maximum (FWHM) of the diffraction peak, respectively. When the material was deposited on Si substrates because of high temperature nearly 250° C, there is no peak related to TiO_2:rGO. According to the JCPDS file the lattice parameter values are a = 4.590 A° and c = 3.239 A°. The calculated values of these diffractions were well matched with the results which are shown in Figure 2(a-b).

Table 1: Structural studies of TiO_2: rGO coated on glass substrates and Si substrates

Sample	Lattice parameter A°		Crystal Size (nm)	Strain 10^{-4}	Dislocation density × 10^{14} lines/m²
TiO_2:rGO deposited on glass substrates	a = 4.352	c=2.786	56	3.106	6.994
TiO_2:rGO deposited on Si substrates	4.251	2.699	72	3.256	7.0125

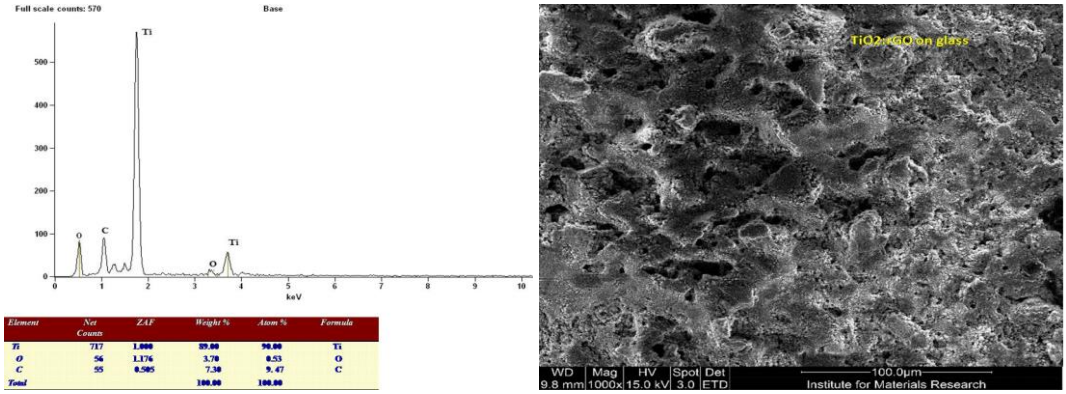

Figure 3(a-b): SEM with EDAX Analysis of TiO_2:rGO coated on glass substrates

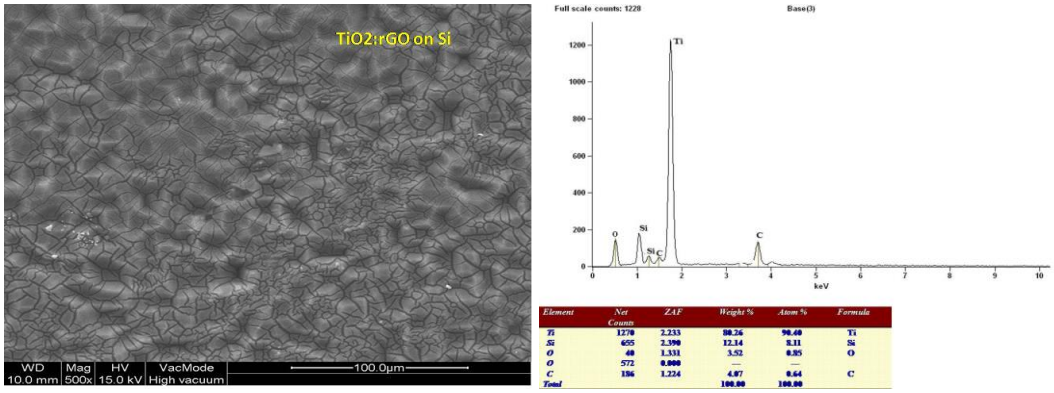

Figure 4(a-b): SEM with EDAX Analysis of TiO_2:rGO coated on Si substrates

To fabricate the solar cells the characteristics are (i) Conversion efficiency (ii) Fill factor (iii) Open circuit voltage and (iv) Short circuit current. The conversion efficiency of solar cell is given by

Conversion efficiency =

$$\frac{Poweroutput}{Incidentengery} \times 100\% \text{---------(2)}$$

Fill factor = $$\frac{V_m I_m}{V_{oc} I_{Sc}} \text{ ----------(3)}$$

Where V_m – Output voltage at the optimum operating point

I_m – Output current at the optimum operating point

V_{oc} –Open circuit voltage

I_{Sc} – Short circuit current

When the PN junction diode is open circuited, the accumulation of electron and holes on the two sides of the junction, gives rise to open circuit voltage V_0. If a load resistance is connected across the diode, a current will flow in the circuit. The maximum current, called the short circuit current is obtained when an electric short is connected across the diode terminals [13].

The intensity of both these bands decreased from TiO_2: rGO doped material deposited on glass substrates, thereby demonstrating that the bare TiO_2: rGO NPs on glass substrates were more hydroxylated than the surface of TiO_2: rGO NPs on Si substrates. Figure 3(a-b) show typical SEM microstructures of fully dense TiO_2: rGO doped material deposited on glass substrate. At least 400 grains of the picture were measured manually for the estimation of grain size. On visual observation, morphology of these agglomerated particles is dispersed and the fracture mechanism appears to be intergranular. The individual grain size range is about 50–100 nm. TiO_2: rGO doped material deposited on Si substrates have shown that pure tetragonal cubic phases can be stabilized when the crystallite size is

below a critical size primarily due to very low surface energy associated with it shown in figure 4(a-b). When the crystallite size exceeds this size, the transformation of metastable phases to the monoclinic one occurs due to decrease in surface energy.

The EDAX was recorded in the binding energy region of 0–20 keV is shown in figures 4b and 5b. The peak from the spectrum reveals the presence of Ti and O at its keV respectively are listed in the insert tables. The atomic % of Ti and O is for the two different substrates were varied with respect to the compositions and parameters were having the changes accordingly. The present composition of Ti and O reveals that, the formation of non-stoichometric TiO_2 which is superior for photocatalytic applications.

To obtain a better understanding of the formation and shape evolution of TiO_2: rGO doped material deposited on glass substrates HRTEM investigations were carried out. The particle size and morphology were studied using Transmission Electron Microscopy (TEM). The average size determined agreed with the result obtained from XRD analysis. Figure 5(a-b) shows the variation in particle size distribution for TiO_2: rGO doped material deposited on glass substrates. The bright-field image shown in Figure 6(a-b) confirms that particles are in tube shape and the distribution of particle size is relatively narrow. The average size of nanoparticles estimated from TEM micrographs (~50 nm) is in close agreement with that obtained from XRD line broadening analysis, which supports the formation of TiO_2: rGO doped material. Multiple rings are seen in the SAED spectrum, as expected from the XRD pattern [14].

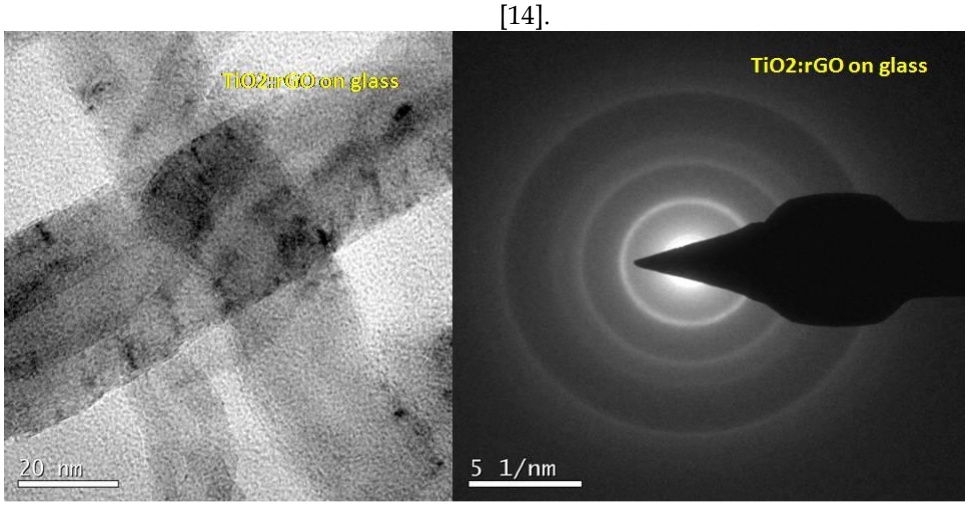

Figure 5(a-b): TEM with SAED pattern Analysis of TiO_2:rGO coated on glass substrates

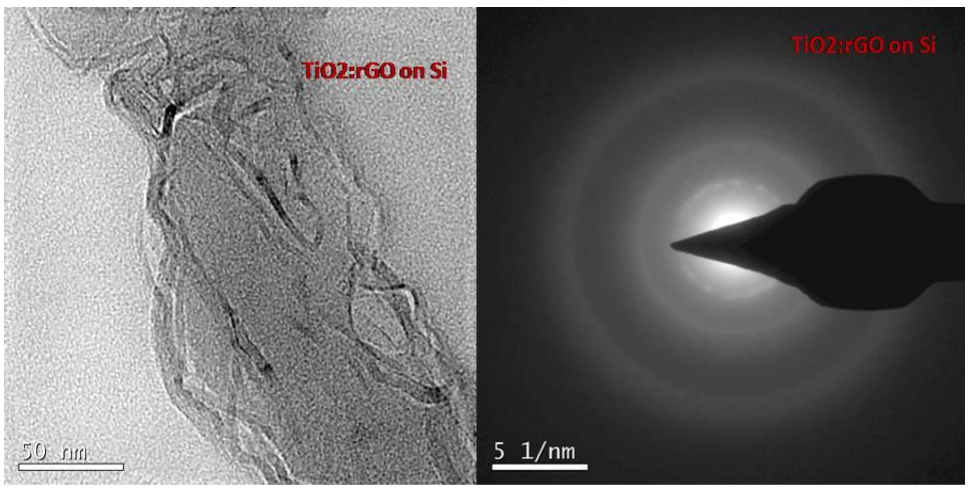

Figure 6(a-b): TEM with SAED pattern Analysis of TiO_2:rGO coated on Si substrates

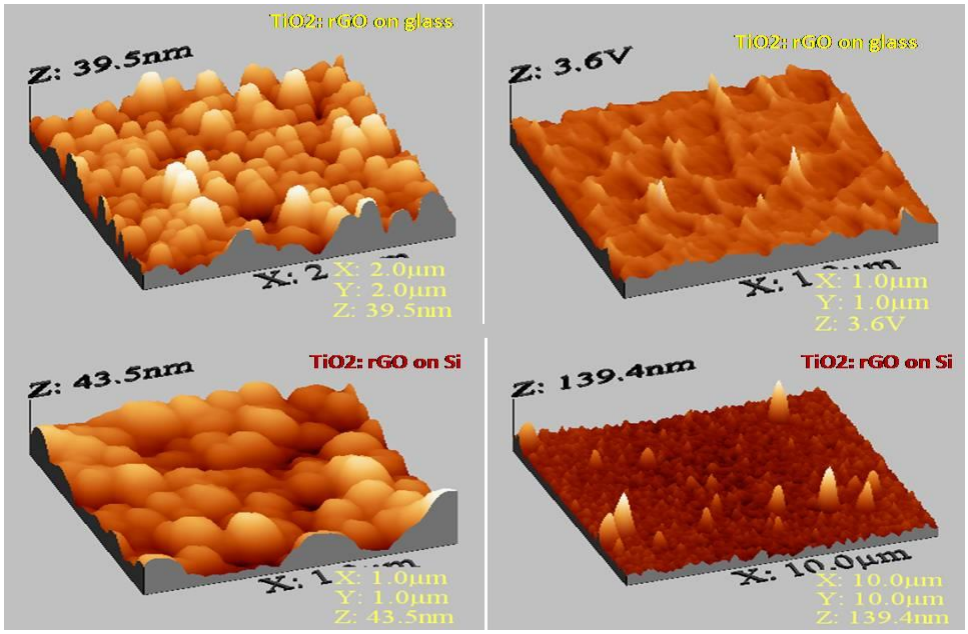

Figure 6(a-b): 2D and 3D AFM analysis of TiO_2:rGO coated on glass substrates
Figure 7(a-b): 2D and 3D AFM analysis of TiO_2:rGO coated on Si substrates

The beginning of constructive grain structure on the surface is visible only TiO_2: rGO doped material on glass and Si susbtrates. AFM images can also be used to find out the surface roughness of the crystal by noting the height deviations from the least fitted line on the 2D and 3D micrograph. Height calibrations were performed using the step heights of freshly cleaved TiO_2: rGO doped material on glass and Si substrates. Due to the super-roughness of the samples, sometimes the laser interference pattern along the slow-scan axis was hard to avoid, which is more notice-able in large-area scanning and has a period of twice the wavelength of the laser [15]. This is caused by the constructive interference of laser reflected from the sample surface and that reflected from the cantilever. The two samples work was investigated by the micromechanical behavior of TiO_2: rGO doped material on glass and Si susbtrates were mechanically exfoliated and transferred of this glass (I Method) and Si susbtrate (II Method), which were covered with 1.04 µm of thermal oxide. We identified the single and spherical shaped by the color influence in the optical microscope, TiO_2: rGO doped material on glass and Si susbtrates were imaged by the atomic force microscopy (AFM) to ensure the uniformity of the surface layer.

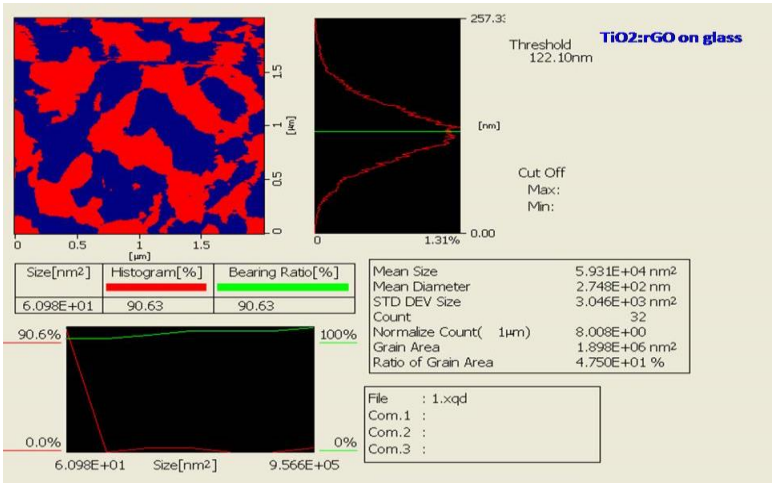

Figure 7: AFM Histogram of TiO_2:rGO coated on glass substrates

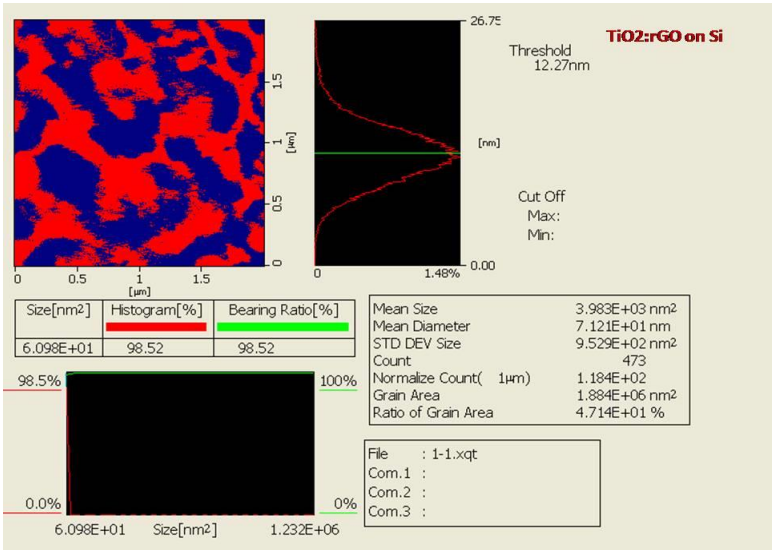

Figure 8: AFM Histogram of TiO_2:rGO coated on Si substrates

In figures 8 and 9 shows the notable Histogram AFM images of TiO_2: rGO doped material on glass and Si susbtrates which represents the formation of different grain size variation as observed from their representative corresponding Histogram graph of the images. This image is representing the roughness nature of the samples clearly.

Next to this the surface morphology of the entitled compound reflecting the similar topography as such as evidenced by AFM images. Here the sharp crust in the AFM images indicating that samples has the potential with reactive edges obviously. Images with two different substrates illustrated in Figure 7 and 8.

Current Voltage (I-V) Measurement

The large area Si solar cells are to be characterized for their ability to convert solar light energy into electrical energy. For this, the junction behavior under illumination is studied. The experimental set up used to measure the I-V characteristics of the TiO_2: rGO doped on the glass and TiO_2: rGO doped on the Si substrate solar cell consists of three main parts. The first part is the solar cell holder. As the active area of the cell, i.e the area over which light is illuminated, is about 100 cm^2 the contacts acting as the positive (+ve) and negative (-ve) terminals should be carefully taken. A special cell holder is made. A copper plated PC Board is used over which the TiO_2: rGO doped on the glass and TiO_2: rGO doped on the Si substrate solar cell is placed which acts as the +ve terminal. Two thick copper strips with tips are used as the negative terminal which makes very good ohmic contacts with the two silver top grids with leads.

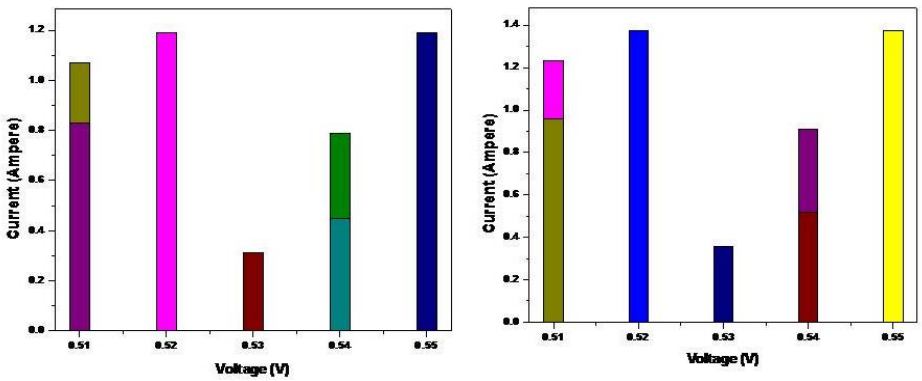

Figure 10(a-b): Voltage and current characteristics of TiO_2:rGO coated on glass and Si substrates

The second part is the illuminating light source which can change the intensity of illumination from 10 to 100 mW/Cm². The lamp (GE-LEH) power is 300 Watts operating at 120 V and has a reflector to produce a highly concentrated white light on to the surface of solar cell. The spectral distribution of this lamp nearly matches the solar spectrum with most of the light intensity is distributed in the visible region 400 to 700 nm. The intensity is measured using Suryamapi intensity meter mW/cm² [16]. The third part is the I-V measuring electrical circuit. It consists of a variable load (resistance box) connected in series with the solar cell through multimeter for measuring the current.

The voltage developed under illumination is measured across this load. The I-V values are taken under different illumination intensity by varying the load resistance and curves are drawn shown in Figure 5a and 5b. The values are tabulated in Table 1 and Table 2. The illuminated I-V curves obtained under varying bias voltages are used to study the junction properties of the TiO_2:rGO doped on glass and TiO_2:rGO doped on the Si solar cells using the following equations.

Table 2: Solar cell fabricated by using TiO_2:rGO coated on glass substrates

Time	Intensity mW/cm²	Voltage (V)	Current (A)	Power (W)
10.00	80	0.52	1.19	0.62
10.30	92	0.55	0.70	0.4
11.00	84	0.55	0.73	0.41
11.30	100	0.55	0.73	0.40
12.00	100	0.51	1.07	0.55
12.30	98	0.53	1.29	0.68
1.00	94	0.55	1.19	0.65
1.30	88	0.55	1.14	0.63
2.00	24	0.51	0.83	0.42
2.30	76	0.53	1.05	0.56
3.00	36	0.53	0.31	0.16
3.30	46	0.53	0.87	0.46
4.00	40	0.54	0.79	0.43
4.30	20	0.54	0.97	0.52

For all practical purposes, a single diode model can be used to fit the I-V data of a solar cell under dark as well as under illumination.

$$I = I_0 \exp \frac{\{q(V - Irs) - 1\} - I_{ph}}{AKT} \text{ ----------(4)}$$

Under open circuit conditions I= 0 and I_{ph} also becomes zero giving rise to derivation for V_{oc} as

$$V_{oc} = \frac{AKT}{q}\left[\ln\left(\frac{I_{ph}}{I_o} + 1\right)\right] \text{ --------(5)}$$

Here I_{ph} is equivalent to the short circuit current $\mathbf{I_{sc}}$ when a graph is drawn beween $\boldsymbol{ln}I_{sc}$ and V_{oc} a straight line is obtained. Its slope and the intercept at $\ln I_{sc}$ axis give the diode quality factor value A and the dark reverse saturation current $\mathbf{I_o}$ respectively.

Table 3: Solar cell fabricated by using TiO_2:rGO coated on Si substrates

Time	Intensity mW/cm²	Voltage (V)	Current (A)	Power (W)
10.00	80	0.55	0.81	0.42
10.30	92	0.55	1.70	0.55
11.00	84	0.55	0.93	0.33
11.30	100	0.55	0.97	0.42
12.00	98	0.54	1.47	0.58
12.30	98	0.53	1.39	0.54
1.00	96	0.55	1.20	0.61
1.30	90	0.55	1.16	0.65
2.00	36	0.54	0.93	0.39
2.30	76	0.54	1.05	0.46
3.00	24	0.53	0.41	0.26
3.30	46	0.53	0.97	0.36
4.00	40	0.54	0.89	0.33
4.30	20	0.55	0.87	0.62

The fill factor (FF) is given as

$$FF = \frac{V_{mp} I_{mp}}{V_{oc} I_{sc}} \quad \text{----------(6)}$$

And the conversion efficiency is computed from the following equation

$$\eta = \frac{V_{oc} I_{sc}}{P_{input}} xFFx100\% \quad \text{----------(7)}$$

The obtained I-V characteristics are shown in Figure 10a. Lowest current density is 11.34 mA/cm^2, compared to other materials. This performance may be due to its low electron and hole mobilities 2 x 10^{-1} cm^2/Vs, which affects the charge collection. It exhibited FF as 61.25% and V_{oc} as 0.56 V. These parameters lead to a power conversion efficiency of 12.56 %. The resulting parameter compared with glass on Si substrate is shown in Figure 10b. The current density is 16.58 mA/cm^2, compared to the glass substrate coating this current density is high, FF of the sample is 72.35% and efficiency is 14.98%. This means an enhancement in the solar cell performance is good compared to the case of using TiO_2:rGO coated on Si substrates than deposited on glass susbtrates [17].

Conclusion

The I-V characteristics for two substrates are varied the FF is nearly 61.25% and 72.35% respectively. The TiO_2:rGO deposited on glass and Si substrates were having the crystal sizes of 56 nm and 72 nm. Sharp crust in the AFM images indicating the composition and surface morphology of the samples. AFM histogram of height calibrations were performed using the step heights of freshly cleaved TiO_2: rGO doped material on glass and Si substrates. Conversion efficiency, Fill factor, Open circuit voltage and Short circuit current were studied. Performance of variation of Intensity, Voltage, Current and Power of the samples deposited on glass and Si substrates were reported

References

1. Prabhavathi, G., Mohamed Saleem, A., Ayeshamariam, A., Karunanithy, M. and Jayachandran, M., "Preparation and characterizations of Graphene oxide and Graphene NPs". *International Journal of Bio-Pharma Research* 8.2 (2019): 2486-2490.
2. Headley, Oliver. "Renewable energy technologies in the Caribbean". Solar Energy 59. 1-3 (1997) : 1-9. Elsevier.
3. Bansal, N.K. and Uhlemann, R., "Development and testing of low-cost solar energy collectors for heating air". Solar energy, 33.2 (1984): 197-208. Elsevier.
4. Marikkannu, S., Kashif, M., Sethupathy, N., Vidhya, V.S., Shakkthivel Piraman, Ayeshamariam, A., Bououdina, M., Naser Ahmed, M. and Jayachandran, M. "Effect of substrate temperature on indium tin oxide (ITO) thin films deposited by jet nebulizer spray pyrolysis and solar cell application." Materials Science in Semiconductor Processing 27 (2014): 562-568. Elsevier.
5. Nivetha, S., Perumalsamy, R., Ayeshamariam, A., Srinivasan, M.P. and Mohamed Saleem, A., "Cadmium Doped with Selenides and Telluride for Photovoltaic Applications: A Review". Fluid Mech Open Acc, 4.167 (2017): 2476-2296. OMICS International.
6. Perumalsamy, R., Prabhavathi, G., Nivetha, S., Mohamed Saleem, A. and Karunanithy, M., "Study of Nanomaterials Prepared by Combustion Method Using High Heat Combustion Chamber and Agreement with the Reported Results". Fluid Mech Open Acc, 4.175 (2017): 2476-2296. OMICS International.
7. El-Bery, H.M., Matsushita, Y. and Abdel-moneim, A. "Fabrication of efficient TiO_2-RGO heterojunction composites for hydrogen generation via water-splitting: Comparison between RGO, Au and Pt reduction sites". *Applied Surface Science, 423* (2017)*:* 185-196. Elsevier.
8. Brabec, C.J. "Organic photovoltaics: technology and market". *Solar energy materials and solar cells*, *8*.2-3(2004):.273-292. Elsevier.
9. Kippelen, B. and Brédas, J.L. "Organic photovoltaics". *Energy & Environmental Science*, 2.3 (2009):251-261. Royal Society of Chemistry.
10. Bundgaard, E. and Krebs, F.C. "Low band gap polymers for organic photovoltaics". *Solar Energy Materials and Solar Cells*, *91*.11(2007): 954-985. Elsevier.
11. Saleem, A.M., Prabhavathi, G., Karunanithy, M., Ayeshamariam, A. and Jayachandran, M. "Green Synthesis of Nanoparticle by Plant Extracts—A New Aproach in Nanoscience".

Journal of Bionanoscience, *12*.3 (2018):401-407. American Scientific Publishers.

12. Günes, S., Neugebauer, H. and Sariciftci, N.S., "Conjugated polymer-based organic solar cells". Chemical reviews, 107.4 (2007): 1324-133. ACS Publications.

13. Thompson, B.C. and Fréchet, J.M., "Polymer–fullerene composite solar cells". A Journal German Chemical Society, 47.1 (2008): 58-77. Angewandte Chemie International Edition.

14. Prabhu, S., Cindrella, L., Kwon, O.J. and Mohanraju, K., "Superhydrophilic and self-cleaning rGO-TiO_2 composite coatings for indoor and outdoor photovoltaic applications". *Solar Energy Materials and Solar Cells*, *169*(2017) : 304-312. Elsevier.

15. Hasan, M., Lai, C.W., Bee Abd Hamid, S. and Jeffrey Basirun, W. "Effect of Ce doping on RGO-TiO_2 nanocomposite for high photoelectrocatalytic behavior". *International Journal of Photoenergy*, *2014* (2014): 1-8 Handawi Publishing Corporation.

16. El-Bery, H.M., Matsushita, Y. and Abdel-moneim, A., "Fabrication of efficient TiO_2-RGO heterojunction composites for hydrogen generation via water-splitting: Comparison between RGO, Au and Pt reduction sites". *Applied Surface Science*, *423* (2017): 185-196. Elsevier.

17. Cheng, C., Karuturi, S.K., Liu, L., Liu, J., Li, H., Su, L.T., Tok, A.I.Y. and Fan, H.J., "Quantum-Dot-Sensitized TiO_2 Inverse Opals for Photo Electrochemical Hydrogen Generation". *Small*, *8*.1(2012): 37-42. Wiley.

Cite this article as:

Prabhavathi G., Anuradha N., Afroos Banu A., Ayeshamariam A., Punithavelan N., Mohamed Saleem A. and M. Jayachandran. Performance of Solar cell fabricated using TiO_2: rGO on glass and Si substrates prepared by Thermal Evaporation Technique. *International Journal of Bio-Pharma Research*, Volume 8, Issue 3 (2019) pp. 2504-2513.

http://dx.doi.org/10.21746/ijbpr.2019.8.3.3

Source of support: Nil; **Conflict of interest:** Nil.